Comparative Study of Fundamental Properties of Honey Comb Photonic Crystal Fiber at 1.55µm Wavelength

[*]S.S. Mishra and [#]Vinod Kumar Singh
Department of Applied Physics
I. S. M., Dhanbad-826004, India
[*]Suvendumohan_2006@yahoo.co.in
[#]singh.vk.ap@ismdhanbad.ac.in

Abstract—**Fundamental properties such as mode field distribution, real effective refractive index, imaginary effective refractive index, confinement loss of two new kinds of honeycomb photonic crystal fibers are successfully studied by using Full-Vectorial Finite element method (FV-FEM). Low confinement loss 0.1×10^{-4}dB/km is achieved at wavelength 1.55µm in hollow core honey comb PCF by removing 6-air holes in cladding region with air hole diameter 1.38µm in cladding region, pitch 2.3µm and air core diameter 0.2µm.**

***Index Terms*— Honey comb Photonic crystal fiber, Full-Vectorial Finite Element Method, Effective refractive index, modal field pattern, confinement loss.**

I. INTRODUCTION

Recently, Photonic Crystal fibers (PCFs) have diverse applications in supercontinuum generation, nonlinear optics, telecommunications, sensors, soliton, lasers, medical instrumentations etc [1-5]. Photonic crystal fibers can be divided into two modes of operation, according to their mechanism for confinement. Those, with a solid core or a core with a higher average index than the microstructured cladding, can operate on the same guiding principle as conventional optical fiber called as solid core PCF[6]. Alternatively, one can create a defect by introducing an air hole in core region which is also known as hollow core PCF where light can confine in a lower-index core and even a hollow (air) core and light is confined by a photonic band gap effect. Potential advantage of a hollow core is that one can dynamically introduce materials into the core, such as a gas that is to be analyzed for the presence of some substance. However, they can have a much higher effective-index contrast between core and cladding and therefore can have much stronger confinement for applications in nonlinear optical devices, polarization-maintaining fibers. In particular, when the defect is formed by removing several air holes in cladding region of PCF the structure becomes honeycomb PCF. If we introduce a small air core as defect in core region of honeycomb PCF we call it as hollow core or air-guiding PCF. In this fiber, light guiding mechanism is due to completely photonic band gap effect[7]. For designing Photonic band gap fibers (PBGFs),

Brazilian Microwave and Optoelectronics Society-SBMO *received 11 May 2011; for review 13 May 2011; accepted 23 Sept. 2011*
Brazilian Society of Electromagnetism-SBMag *ISSN 2179-1074*

not only the core structure but also the cladding structure is very important. When large band-gaps are obtained in the cladding, the fiber can possess desirable properties such as a low confinement loss and a broadband transmission range. Generally, a triangular lattice for the cladding structure is used for realizing airguiding PBGFs because of its large band-gaps. So a honeycomb structures for air-guiding PBGFs with large band-gaps have also been proposed [8, 9] and have gathered much attention. In addition, a modified honeycomb structure has been investigated by Broeng et al.[10]. However it has been evaluated only how the presences of interstitial air holes affect the bandgap properties. More recently, Chen et al suggested the possibility that the modified honeycomb structure produces completely different large band-gaps beyond the realm of triangular and honeycomb lattices as structural parameters are adjusted [11]. Saitoh et al [12] and Vincetti et al [13] calculated a modal dispersion curve and confinement loss properties for modified honey comb type air guiding PBGFs with large core diameters, which suffers from multi-mode transmission. However, the possibility of realizing single-mode air-guiding PBGFs operating in a wide wavelength range with low confinement losses has not been investigated so far. Confinement loss is the important issues in optical communication through optical fiber [14]. Recently, different kinds of PCFs have been designed by taking appropriate geometrical parameters such as air hole diameter, pitch and air core diameter with various propagation properties e.g. dispersion, birefringence, confinement loss, nonlinearity etc [15,16]. Confinement loss in conventional optical fiber is very high. To overcome these limitations of conventional optical fiber an alternate fiber e.g. hollow core honey comb photonic crystal fiber is developed. Due to complex structure of PCF, different numerical techniques has been used by researchers to study the different properties of PCF such as Finite Element Method (FEM) by Brechet et.al in 2000 [17], Multipole Method (MM) by White et.al [18], Finite Difference Time Domain Method (FDTDM) by Qiu et.al [19], Plane Wave Expansion Method (PWEM) by Guo et.al [20], Effective index Method by Chiang et.al [21], Vector wave Expansion method by Issa et.al [22], Time domain beam propagation method by Koshiba et.al [23] and Localized function Method by Mogilevtsev et.al [24] and other numerical modeling.

Finite element methods are divided into two catagory one is Scalar FEM and another is Full-vectorial FEM. Scalar FEM technique is used only for solving nodal element but it fails to solve edge element in the domain where as FV-FEM technique is used to solve both nodal element as well as edge element in the domain. Here we have used FV-FEM, which is suitable for such analysis as it can handle complicated structure geometries and also takes less computational time. Two new types of hexagonal triangular-based cladding structure PCF are used, where refractive index of air and silica are 1 and 1.45 respectively. By manipulating circular air hole diameter 'd', pitch 'Λ' and air core diameter d_c , it is possible to control the properties of PCF such as real effective refractive index, imaginary effective refractive index, confinement loss, at wavelength 1.55μm.

II. FULL-VECTORIAL FINITE ELEMENT METHOD

The Full Vectorial Finite element method (FEM) is generally advantageous in complex geometries of photonic crystal fiber. It is a full vector implementation for both propagation and leaky modes and cavity modes for two dimensional Cartesian cross sections in cylindrical co-ordinates. First and second order interpolant basis are provided for each triangular elements. PEC (Perfect electrical conductor) or PML (perfectly matched layer) boundary conditions is employed at computational domain for evaluating total dispersion and confinement loss of proposed PCF [25].

Brazilian Microwave and Optoelectronics Society-SBMO received 11 May 2011; for review 13 May 2011; accepted 23 Sept. 2011
Brazilian Society of Electromagnetism-SBMag *ISSN 2179-1074*

Under the source free condition time dependent Maxwell's curl equation can be expressed a

$$\nabla \times E = -j\omega\mu_0[\mu_r]H \tag{1}$$

$$\nabla \times H = j\omega\mathcal{E}_0[\mathcal{E}_r]E \tag{2}$$

Where ω is the angular frequency,μ_0 and $\mathcal{E}_0$ are the permeability and permittivity of free space, and $[\mu_r]$ and $[\mathcal{E}_r]$ are, respectively the relative permeability and permittivity tensors of the medium given by

$$[\mu_r] = \begin{bmatrix} \mu_{xx} & \mu_{xy} & \mu_{xz} \\ \mu_{yx} & \mu_{yy} & \mu_{yz} \\ \mu_{zx} & \mu_{zy} & \mu_{zz} \end{bmatrix} \tag{3}$$

$$[\mathcal{E}_r] = \begin{bmatrix} \mathcal{E}_{xx} & \mathcal{E}_{xy} & \mathcal{E}_{xz} \\ \mathcal{E}_{yx} & \mathcal{E}_{yy} & \mathcal{E}_{yz} \\ \mathcal{E}_{zx} & \mathcal{E}_{zy} & \mathcal{E}_{zz} \end{bmatrix} \tag{4}$$

From Equation (1) and (2), we can derive the vectorial wave equation as

$$\nabla \times ([P]\nabla \times \phi) - k_0^2[q]\phi = 0 \tag{5}$$

Where $k_0 = \omega\sqrt{\mu_0}\mathcal{E}_0$ is the wave number in free space, ϕ is either the electric field E or the magnetic field H, and the tensor $[p]$ and $[q]$ are given by

$$[p] = \begin{bmatrix} p_{xx} & p_{xy} & p_{xz} \\ p_{yx} & p_{yy} & p_{yz} \\ p_{zx} & p_{zy} & p_{zz} \end{bmatrix} = \begin{bmatrix} \mu_{xx} & \mu_{xy} & \mu_{xz} \\ \mu_{yx} & \mu_{yy} & \mu_{yz} \\ \mu_{zx} & \mu_{zy} & \mu_{zz} \end{bmatrix}^{-1} \tag{6}$$

$$[q] = \begin{bmatrix} q_{xx} & q_{xy} & q_{xz} \\ q_{yx} & q_{yy} & q_{yz} \\ q_{zx} & q_{zy} & q_{zz} \end{bmatrix} = \begin{bmatrix} \mathcal{E}_{xx} & \mathcal{E}_{xy} & \mathcal{E}_{xz} \\ \mathcal{E}_{yx} & \mathcal{E}_{yy} & \mathcal{E}_{yz} \\ \mathcal{E}_{zx} & \mathcal{E}_{zy} & \mathcal{E}_{zz} \end{bmatrix} \tag{7}$$

For ϕ=E and

$$[p] = \begin{bmatrix} p_{xx} & p_{xy} & p_{xz} \\ p_{yx} & p_{yy} & p_{yz} \\ p_{zx} & p_{zy} & p_{zz} \end{bmatrix} = \begin{bmatrix} \mathcal{E}_{xx} & \mathcal{E}_{xy} & \mathcal{E}_{xz} \\ \mathcal{E}_{yx} & \mathcal{E}_{yy} & \mathcal{E}_{yz} \\ \mathcal{E}_{zx} & \mathcal{E}_{zy} & \mathcal{E}_{zz} \end{bmatrix}^{-1} \tag{8}$$

$$[q] = \begin{bmatrix} q_{xx} & q_{xy} & q_{xz} \\ q_{yx} & q_{yy} & q_{yz} \\ q_{zx} & q_{zy} & q_{zz} \end{bmatrix} = \begin{bmatrix} \mu_{xx} & \mu_{xy} & \mu_{xz} \\ \mu_{yx} & \mu_{yy} & \mu_{yz} \\ \mu_{zx} & \mu_{zy} & \mu_{zz} \end{bmatrix} \tag{9}$$

For ϕ=H

In this chapter we have considered 2-dimension photonic crystal fiber with triangular lattice which are uniform along the z direction and periodic in the x-y plane. The field distribution ϕ of the wave modes in plane propagation can be expressed as

$$\phi(x, y, z) = \phi_t(x, y) + \hat{z}\phi_z(x, y) \tag{10}$$

Where ϕ_t and ϕ_z, both assumed to be function of x and y, are the transverse and longitudinal field components of ϕ, respectively. Substituting Eq. (10) into Eq. (5) and using

$$\nabla = \nabla_t + \nabla_z \tag{11}$$

Brazilian Microwave and Optoelectronics Society-SBMO *received 11 May 2011; for review 13 May 2011; accepted 23 Sept. 2011*
Brazilian Society of Electromagnetism-SBMag *ISSN 2179-1074*

Where ∇_t and ∇_z are, respectively, the transverse and longitudinal parts of ∇ operator. Eq.(8) can be separated into its transverse component

$$\nabla_t \times \left(\begin{bmatrix} 0 & 0 & 0 \\ 0 & 0 & 0 \\ 0 & 0 & p_{zz} \end{bmatrix} \nabla_t \times \phi_t + \begin{bmatrix} 0 & 0 & 0 \\ 0 & 0 & 0 \\ p_{zx} & p_{zy} & 0 \end{bmatrix} \nabla_t \times \hat{z}\phi_z \right)$$
$$-k_0^2 \left(\begin{bmatrix} q_{xx} & q_{xy} & 0 \\ q_{yx} & q_{yy} & 0 \\ 0 & 0 & 0 \end{bmatrix} \phi_t + \begin{bmatrix} 0 & 0 & q_{xz} \\ 0 & 0 & q_{yz} \\ 0 & 0 & 0 \end{bmatrix} \phi_z \right) = 0 \quad (12)$$

And its longitudinal component

$$\nabla_t \times \left(\begin{bmatrix} 0 & 0 & p_{xz} \\ 0 & 0 & p_{yz} \\ 0 & 0 & 0 \end{bmatrix} \nabla_t \times \phi_t + \begin{bmatrix} p_{xx} & p_{xy} & 0 \\ p_{yx} & p_{yy} & 0 \\ 0 & 0 & 0 \end{bmatrix} \nabla_t \times \hat{z}\phi_z \right)$$
$$-k_0^2 \left(\begin{bmatrix} 0 & 0 & 0 \\ 0 & 0 & 0 \\ q_{zx} & q_{zy} & 0 \end{bmatrix} \phi_t + \begin{bmatrix} 0 & 0 & 0 \\ 0 & 0 & 0 \\ 0 & 0 & q_{zz} \end{bmatrix} \phi_z \right) = 0 \quad (13)$$

For hybrid node/edge FEM [26], the transverse components are expanded in a vector (edge element) basis.

$$\overrightarrow{E_T}(x,y)e^{-j\beta z} = \sum_{i=1}^{n} \overrightarrow{N_i} E_{Ti} = \sum_{i=1}^{n} \{U\hat{x} + V\hat{y}\} E_{Ti} \quad (14)$$

Where, E_{Ti} are the values of the field along each edge. The longitudinal component (perpendicular to the plane of the element) is represented by a scalar (node element) basis.

$$E_z(x,y)e^{-j\beta z} = \sum_{i=1}^{n} N_i E_{zi} \quad (15)$$

Where, E_{zi} are the values of the field and N_i are the basis at each node. The basis dimension 'n' depends on the geometry of the element and the order of the interpolation. Since the Euler Langrangian equations of the functional correspond to original wave equations the solution of latter equations can be approximated by extremization of the functional [27-31]. The functional are approximated using interpolation of polynomial basis functions and functional are discretized in a finite no. of element within the computational domain.

$$\frac{\partial F}{\partial E_i} = 0 \quad (16)$$

Finally, we will get matrix generalized eigen-value equation of the form

$$\nabla F = \left(A - n_{eff}^2 B\right)\{E_{Ti}\} = \{0\} \quad (17)$$

Where A and B represent global finite matrices, E_{Ti} are Transeverse electric field and n_{eff} represent the modal effective refractive index, $n_{eff}=\beta/k_0$. Here β is the propagation constant for guided mode and k_0 is the propagation constant for free space, $k_0=2\pi/\lambda$.

III. RESULTS AND DISCUSSION

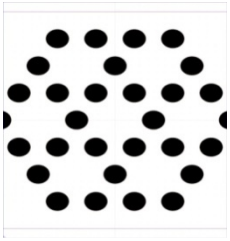

Brazilian Microwave and Optoelectronics Society-SBMO *received 11 May 2011; for review 13 May 2011; accepted 23 Sept. 2011*
Brazilian Society of Electromagnetism-SBMag *ISSN 2179-1074*

Fig. 1(a) Solid Core Honey Comb PCF

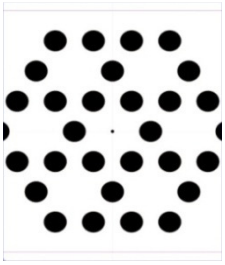

Fig. 1(b) Hollow Core Honey Comb PCF

We have compared fundamental properties of such as mode field distribution, real part and imaginary part of effective refractive index, dispersion and confinement loss properties of two new kinds of honeycomb PCF by using FV-FEM. In our designing for first kind PCFs, 6-air holes are missing in cladding region and one air hole in core region (Solid Core Honey comb PCF) and in another type only 6-air holes are missing in cladding region (Hollow Core Honey Comb PCF). Black regions are air hole and white regions are solid silica as shown in fig 1(a) and 1(b) respectively. For the first kinds of honey comb fiber we have varied air hole diameter d=1.34 µm, 1.36 µm and 1.38 µm respectively for three structures by keeping pitch (2.3 µm) same. For the second kinds of honey comb fiber we have varied air core diameter d_c as 0.05µm, 0.1µm and 0.2µm respectively by taking identical air holes in cladding region and pitch equals to d=1.38 µm and Λ=2.3 µm respectively.

By using FV-FEM simulation technique [32], first we calculated real effective refractive index with wavelength range 0.9 µm to 1.7 µm for first kind of PCFs as shown in Fig.1(a). We observed that real part effective refractive index decreases with increasing air hole diameter as well as increasing wavelength and it is found that real part effective refractive index is 1.413756 at 1.55 wavelength when air hole diameter d=1.38µm as shown in Fig.2(a). For second kind of PCFs, it is found that real part effective refractive index decreases with increasing wavelength and increases with increasing air core diameter and real part effective refractive index is obtained 1.410566 at 1.55µm wavelength when air core diameter is d_c=0.2µm as shown in Fig.2(b).The transverse electric mode field pattern at wavelength 1.55µm of two kinds of PCFs are shown in Fig.3(a) and 3(b) respectively. It shows that mode field pattern is confined more in second kind of PCFs in comparison to 1st kind.

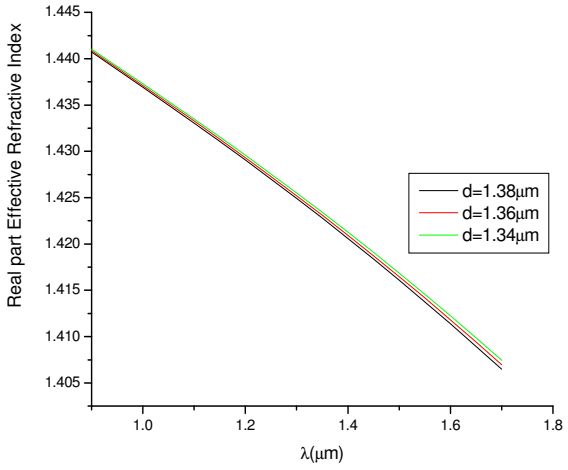

Brazilian Microwave and Optoelectronics Society-SBMO *received 11 May 2011; for review 13 May 2011; accepted 23 Sept. 2011*
Brazilian Society of Electromagnetism-SBMag *ISSN 2179-1074*

Fig.2(a) Variation of Real part effective refractive index with wavelength of Solid core honeycomb PCF having identical air hole diameter d=1.38µm,1.36µm,and 1.34µm of same pitch Λ=2.3µm for all three structures.

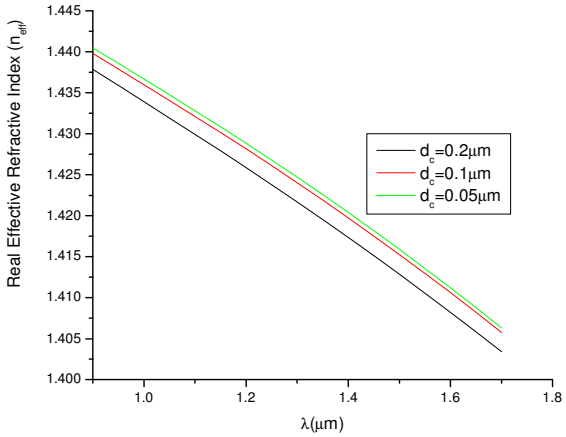

Fig. 2(b) Variation of Real part effective refractive index with wavelength of Hollow core honeycomb PCF having air core diameter d_c=0.2µm,0.1µm,and 0.05µm of same pitch Λ=2.3µm and air hole diameter d=1.38µm for all three structures.

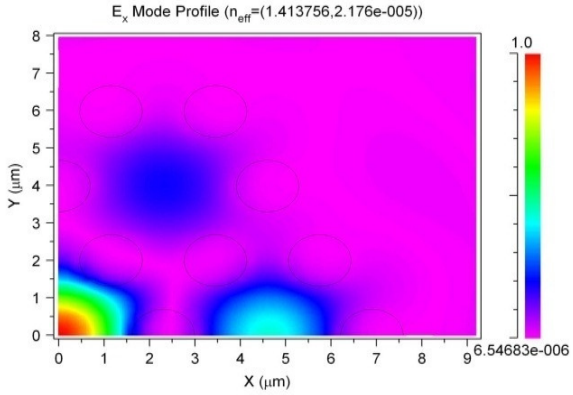

Fig.3(a) Simulated transverse electric modal field pattern (one fourth part) of Solid core honeycomb PCF at wavelength 1.55µm. For structure-1(a) (all air hole diameter d=1.38µm and pitch Λ=2.3 µm)

Brazilian Microwave and Optoelectronics Society-SBMO *received 11 May 2011; for review 13 May 2011; accepted 23 Sept. 2011*
Brazilian Society of Electromagnetism-SBMag *ISSN 2179-1074*

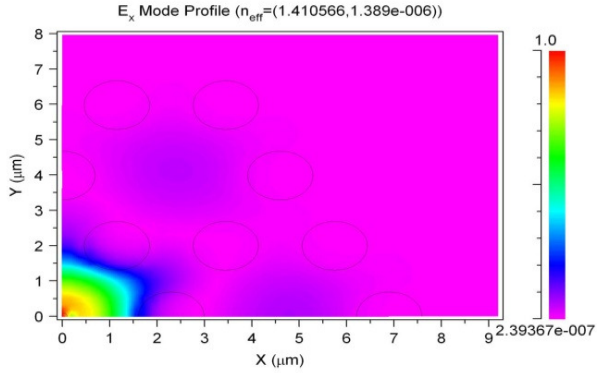

Fig.3(b) Simulated transverse electric modal field pattern (one fourth part) of Hollow core honeycomb PCF at wavelength 1.55μm. For structure-1(b) (air hole diameter in cladding region d=1.38μm, air core diameter d_c=0.2 μm and pitch Λ=2.3 μm)

The variation of effective refractive index with normalized frequency was also studied for different fiber parameter in both cases. As clear from Fig.4(a) and 4(b), the real part effective refractive index increases with increasing normalized frequency and decreases with decreasing air hole diameter in solid core PCF and air core diameter in hollow core PCFs.

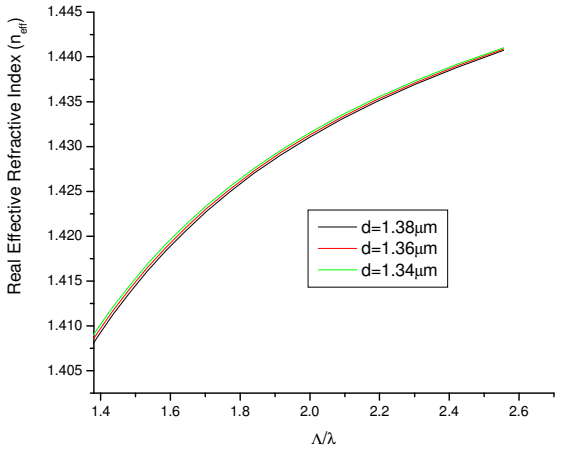

Fig.4(a) Variation of Real part effective index with normalized frequency of Solid core honeycomb PCF having air hole diameter d=1.38μm,1.36μm and 1.34μm of same pitch Λ=2.3μm for all three structures.

Brazilian Microwave and Optoelectronics Society-SBMO *received 11 May 2011; for review 13 May 2011; accepted 23 Sept. 2011*
Brazilian Society of Electromagnetism-SBMag *ISSN 2179-1074*

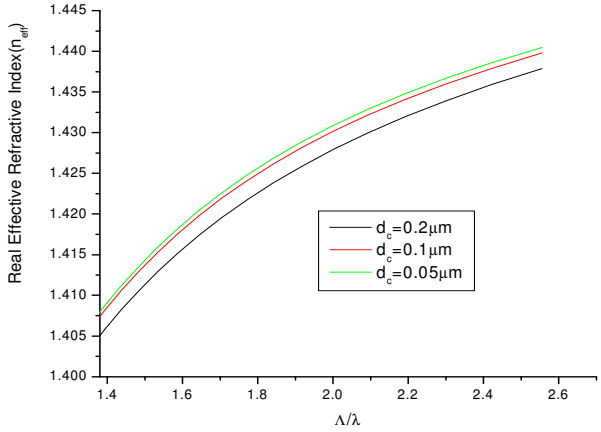

Fig. 4(b) Variation of Real part effective index with normalized frequency of Hollow core honey comb PCF having air core diameter d_c=0.2μm,0.1μm,and 0.05μm of same pitch Λ=2.3μm and air hole diameter d=1.38μm for all three structures.

As clear from Fig.4(a) and 4(b), the real part effective refractive index increases with increasing normalized frequency and decreases with decreasing air hole diameter in solid core PCF and air core diameter in hollow core PCFs.

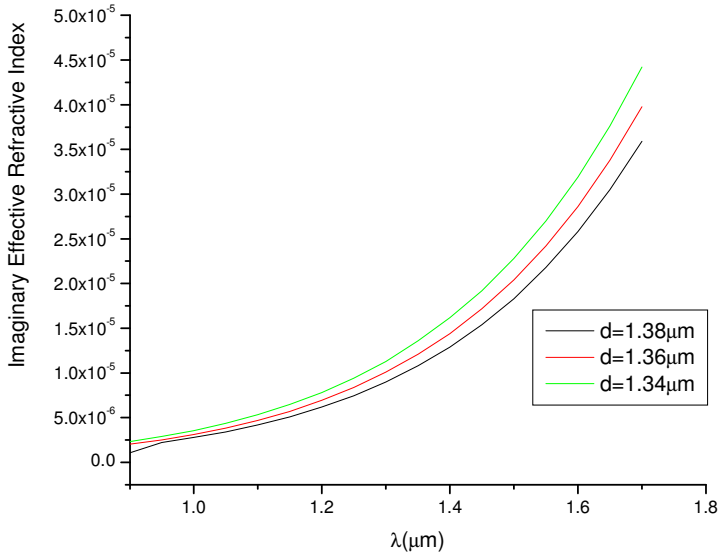

Fig.5(a) Variation of Imaginary part effective refractive index with wavelength of Solid core honeycomb PCF having identical air hole diameter d=1.38μm,1.36μm,and 1.34μm of same pitch Λ=2.3μm for all three structures.

Brazilian Microwave and Optoelectronics Society-SBMO *received 11 May 2011; for review 13 May 2011; accepted 23 Sept. 2011*
Brazilian Society of Electromagnetism-SBMag *ISSN 2179-1074*

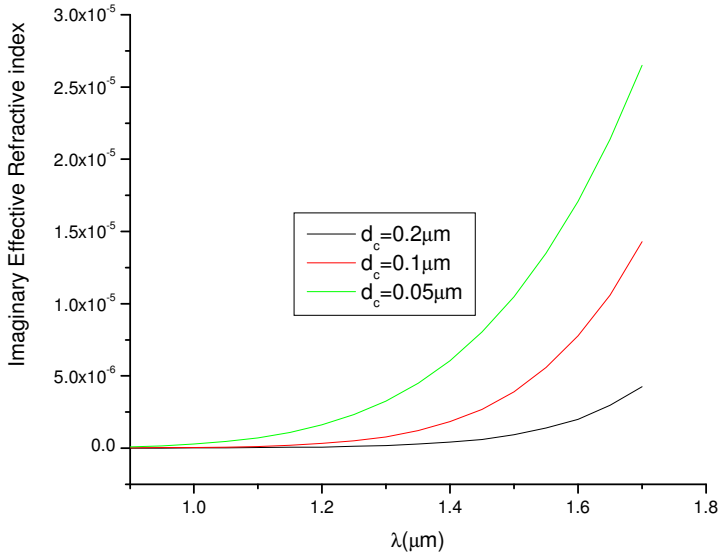

Fig. 5(b) Variation of Imaginary part effective refractive index with wavelength of Hollow core honeycomb PCF having air core diameter d_c=0.2μm,0.1μm and 0.05μm of same pitch Λ=2.3μm and air hole diameter d=1.38μm for all three structures.

Imaginary effective refractive index is an important parameter for analysis confinement loss of PCFs. We calculated imaginary part of effective refractive index corresponding to the same wavelength range for two kinds of PCFs under studied. It is observed that imaginary part of effective refractive index is decreases with increasing air hole diameter and air core diameter. It is also increases with increasing wavelength for all three structures. Imaginary effective refractive index at wavelength 1.55μm is obtained 2.176×10^{-5} when the air hole diameter is 1.38 for first kind PCF and 1.386×10^{-5} is obtained when air core diameter is 0.2μm as shown in Fig. 5(a) and 5(b) respectively.

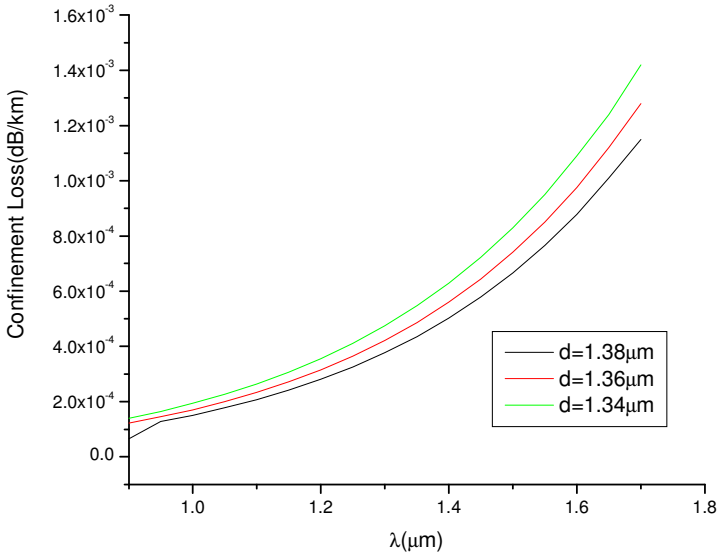

Fig.6(a) Variation of confinement loss with wavelength of Solid core honeycomb PCF having identical air hole diameter d=1.38μm,1.36μm and 1.34μm of same pitch Λ=2.3μm for all three structures.

Brazilian Microwave and Optoelectronics Society-SBMO *received 11 May 2011; for review 13 May 2011; accepted 23 Sept. 2011*
Brazilian Society of Electromagnetism-SBMag *ISSN 2179-1074*

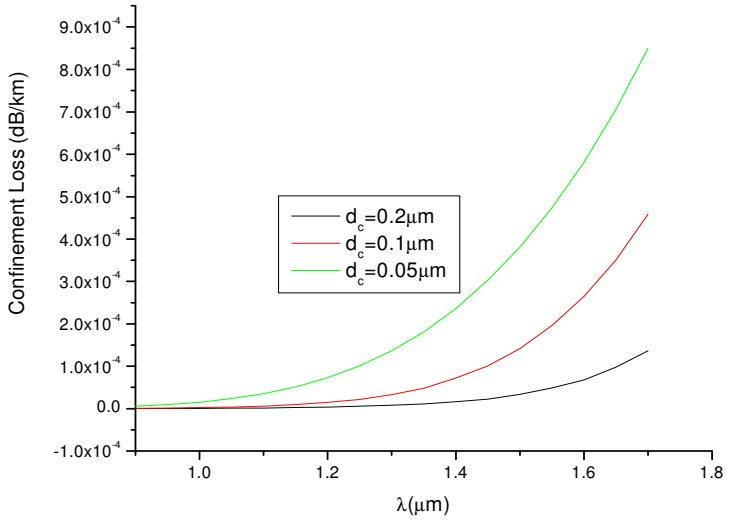

Fig.6 (b) Variation of confinement loss with wavelength of Hollow core honeycomb PCF having air core diameter d_c=0.2μm, 0.1μm and 0.05μm of same pitch Λ=2.3μm and air hole diameter d=1.38μm for all three structures.

After getting imaginary effective refractive index we can easily calculate confinement loss of two kinds of PCFs by using following formula given bellow.

$$\text{Confinement loss} = 8.686\, k_0\, \text{Im}[n_{eff}] \qquad (35)$$

Where $\text{Im}[n_{eff}]$ represented as imaginary effective refractive index and $k_0 = 2\pi/\lambda$, with λ is the propagation wavelength.Once we got imaginary effective refractive index, we can calculate confinement loss of PCF easily by using the equation (35). It is found that confinement loss decreases with increasing air hole diameter and increases with wavelength for two kinds of PCFs as shown in Fig.6(a) and 6(b). It is clear that at wavelength 1.55μm confinement loss is very-very small e.g 0.1×10^{-4}dB/km in hollow core honeycomb PCF in comparison to solid core honey comb PCF.

IV. CONCLUSION

Fundamental properties of two new kinds of Honey comb PCF are studied successfully via FV-FEM simulation technique. The simulation result proves that air holes of the cladding and air core in core region have a strong influence on the PCFs to confinement loss. Hollow core honey comb PCFs having identical air hole diameter d=1.38μm, air core diameter d_c=0.2μm and pitch Λ=2.3μm shows very small confinement loss e.g 0.1×10^{-4}dB/km at wavelength 1.55μm. This kind of PCFs may be used in telecommunication as well as gas sensing purpose.

REFERENCES

[1] J.C. Knight, T. A. Birks, P. St. J. Russell and D. M. Akin, "All-Sillica single mode fiber with photonic crystal cladding," Opt. Letters 21, pp.1547-1549,1996.

[2] R. S. Fyath, Alhuda A. Al-mfrji,"Theoretical investigation of noise and modulation characteristics of photonic crystal lasers," Fiber and Integrated Optics 30,1,pp.45-60, 2011.

Brazilian Microwave and Optoelectronics Society-SBMO *received 11 May 2011; for review 13 May 2011; accepted 23 Sept. 2011*
Brazilian Society of Electromagnetism-SBMag *ISSN 2179-1074*

[3] Sunil K. Khijwania, Frances D. Carter, John T. Foley and Jagdish P. Singh, "Effect of lunching condition on modal power characteristics of multi mode step index optical fiber: A theoretical and Experimental Investigation," Fiber and Integrated Optics 29,1, pp.62-75,2010.

[4] John D. Joannopoulos, Steven G. Johnson, Joshua N. Winn and Robert D. Meade, "Photonic Crystals: molding the flow of light," Princeton University Press Princeton and Oxford, 2008.

[5] J. C. Knight, "Photonic Crystal Fibres," Nature, Vol. 424, pp. 847-851, 2003.

[6] T. P Hansen, et al, "Solid-Core Photonic Bandgap Fiber with Large Anomalous Dispersion", OFC Proceeding, pp.70-77, 2003.

[7] C. M. Smith, N. Venkataraman, M. T. Gallagher, D. Müller, J. A. West, N. F. Borrelli, D. C. Allan, and K.W. Koch, "Low-loss hollow-core silica/air photonic bandgap fibre," Nature 424, 657-659 (2003).

[8] M. Yan and P. Shum, "Air guiding with honeycomb photonic bandgap fiber," IEEE Photon. Technol. Lett.17, 64-66 (2005).

[9] M. Yan, P. Shum, and J. Hu, "Design of air-guiding honeycomb photonic bandgap fiber," Opt. Lett. 30,465-467 (2005).

[10] J. Broeng, S. E. Barkou, A. Bjarklev, J. C. Knight, T. A. Birks, and P. S. J. Russell, "Highly increased photonic band gaps in silica/air structures," Opt. Commun. 156, 240-244 (1998).

[11] M. Chen and R. Yu, "Analysis of photonic bandgaps in modified honeycomb structures," IEEE Photon.Technol. Lett. 16, 819-821, 2004.

[12] K. Saitoh and M. Koshiba, "Leakage loss and group velocity dispersion in air-core photonic bandgap fibers," Opt. Express 11**,** 3100-3109 (2003).

[13] L. Vincetti, F. Poli, and S. Selleri, "Confinement loss and nonlinearity analysis of air-guiding modified honeycomb photonic bandgap fibers", IEEE Photon. Technol. Lett. 18, pp.508-510, 2006.

[14] L. Vincetti, "Confinement Losses in Honeycomb Fiber", IEEE Photon. Tech. Lett. 16, pp. 2048-2050, 2004.

[15] J.Wang, C.J.W. Hu and M.Gao "High birefringence photonic bandgap fiber with elliptical air holes", Optical Fiber Technology 12,pp.265-267, 2006.

[16] Abdur S. M. Razzak and Y.Namihira, "Tailoring Dispersion and Confinement Losses of Photonic crystal fibers using Hybrid Cladding", Journal of Lightwave technology,26,No.13,pp.1909-1914,2008.

[17] F. Brechet, J. Marcou, D. Pagnoux and P. Roy, "Complete Analysis of the characteristics of propagation into photonic crystal fibers by Finite Element Method," Optical Fiber Technology 6, pp. 181-191, 2000.

[18] T. P. White, B. T. Kuhlmey, D. Maystre, G. Renversez, C. Martijn de Sterke, L. C. Botten, "Multipole method for microstructured optical fibers. I. Formulation," J. Opt. Soc. Am. 19, pp.2322-2330, 2002.

[19] M. Qiu "Analysis of guided modes in photonic crystal fibers using the Finite-Differece Time-Domain Method", Microwave and optical Technology Letters 30, pp. 5, 2001.

[20] S. Guo and S. Albin, "Simple plane wave implementation for photonic Crystal calculations," Optics Express 11, pp.167-175, 2003.

[21] K. S. Chiang, "Analysis of rectangular dielectric waveguides: effective-index method with built-in perturbation correction," Electronics Letters 28, pp.388-390, 1992.

Brazilian Microwave and Optoelectronics Society-SBMO *received 11 May 2011; for review 13 May 2011; accepted 23 Sept. 2011*
Brazilian Society of Electromagnetism-SBMag *ISSN 2179-1074*

[22] N. A. Issa and L. Poladian, "Vector wave expansion method for leaky modes of microstructured optical fibers," J. Lightwave Technol. 21, pp.1005–1012, 2003.

[23] M. Koshiba, Y. Tsuji, "Time domain beam propagation method and its application to Applications of Holey Fibre: Joseph Lizier 106 photonic crystal circuits," Journal of Lightwave Technology 18, pp.102-110, 2000.

[24] D. Mogilevtsev, T. A. Birks, P. St. J. Russel, "Localized function method for modeling defect modes in 2-D photonic crystals," Journal of Lightwave Technology 17, pp.2078-2081,1999.

[25] L. Zhao-lun, H. Lan-tian and W. Wei Tailoring Nonlinearity and Dispersion of Photonic crystal Fibers using Hybrid cladding" Brazilian journal of physics 39,1,pp. 50-54. 2009.

[26] H.P. Uranus and J.W. Hoekstr, Modelling of micro structured waveguides using finite element based vectorial mode solver with transparent boundary conditions, Opt. Express 12, 12,pp.2795-2809,2004.

[27] J. Jin, The Finite Element Method in Electromagnetics 2002 (2nd Ed. John Wiley & Sons, New York).

[28] S. S. Mishra and Vinod. K. Singh, Study of Fundamental Propagation Properties of Solid Core Holey Photonic Crystal Fiber in Telecommunication window, Chinese Journal of Physics 48, 5, pp.592-606, 2010.

[29] S. Mishra and Vinod K. Singh, Study of dispersion properties of hollow core photonic crystal fiber by finite element method, Journal of Optoelectronics and Advanced Materials-Rapid Communication 3,ISS 9, pp. 874-878,2009.

[30] S. S. Mishra and Vinod Kumar Singh, Study of Nonlinear Property of Hollow core Photonic crystal fiber," International Journal of Light and Electron Optics 122(8) pp.687-690, 2011.

[31] S. S. Mishra and Vinod K. Singh "Polarization Maintaining Highly Birefringent Small Mode Area Photonic Crystal Fiber at Telecommunication Window," Journal of Microwave Optoelectronics Electromagnetic Research, vol.10, no.1, pp. 33-41, June 2011.

[32] FEMSIM R-Soft Design Group, Ossining 2007. NY 10562,1.3.

Brazilian Microwave and Optoelectronics Society-SBMO *received 11 May 2011; for review 13 May 2011; accepted 23 Sept. 2011*
Brazilian Society of Electromagnetism-SBMag *ISSN 2179-1074*